Geophysical Prospecting

Supporting Information for

What can deep learning-based resolution-improved seismic data do? A case study of faults identification

Lei Lin, Chenglong Li, Yanbin Kuang, Xing Xin, Zhi Zhong

Corresponding Author: Zhi Zhong.
E-mail: zhongzhi@cug.edu.cn

This PDF file includes:

Supporting Information Text

Training Data, Network Architecture, and Training Process of FaultNet

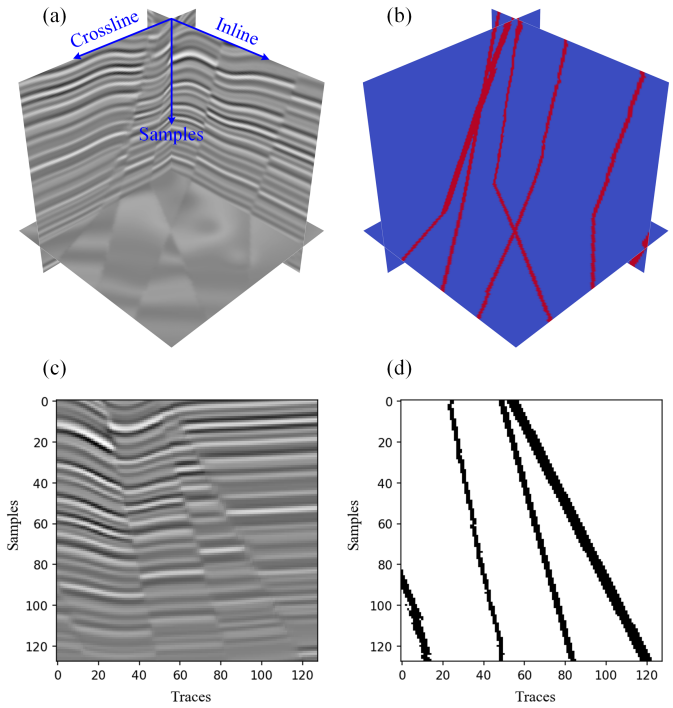

Fig. S1. Seismic volume (a) and its corresponding fault volume (b). (c) is a slice in (a), which is used as input to FaultNet, and (d) is a slice in (b), which is used as the label to FaultNet.

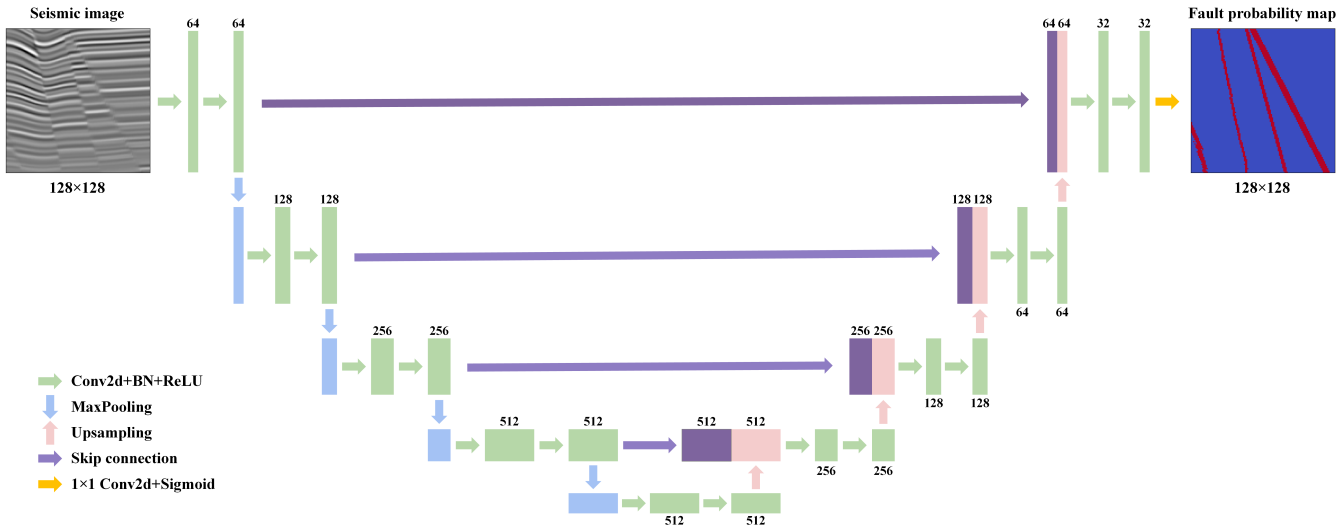

Fig. S2. 2D fault detection neural network based on U-net.

Fig. S3a displays the loss variation on the training (blue line) and validation (red line) datasets with increasing epochs. It can be observed that the validation loss converges to 0.02 after 100 epochs. To quantitatively evaluate FaultNet, we plot the receiver operator characteristic (ROC) (1) curve and calculate the area under the curve (AUC). AUC represents the area under the ROC curve, and its area closer to

one indicates better model performance. The calculated AUC of FaultNet is 0.931, indicating a good fault recognition capability. Fig. S4 displays four examples of fault detection on the validation dataset. Figs. S4a$_{1-4}$ are the normalized seismic images input to FaultNet, Figs. S4b$_{1-4}$ are the fault probability maps predicted by FaultNet, and Figs. S4c$_{1-4}$ are the corresponding fault labels. It can be observed that the predicted fault probabilities match the fault labels very well, with an average intersection over union (IOU) of 0.646 for a threshold of 0.5.

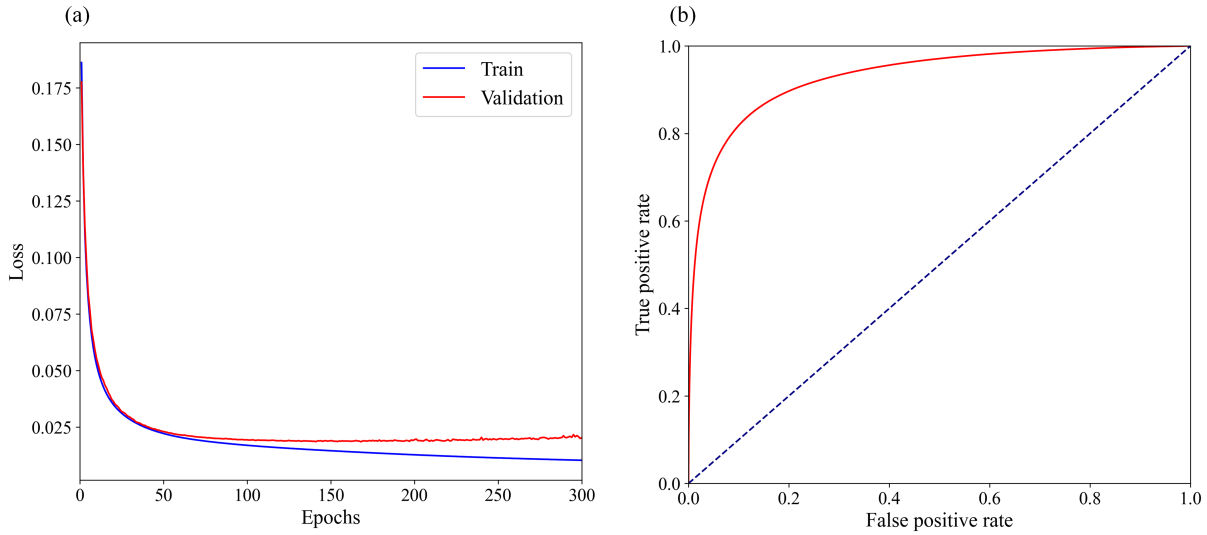

Fig. S3. Loss curve (a) and roc curve (b) of FaultNet.

$4\times$ and $8\times$ Super-Resolution

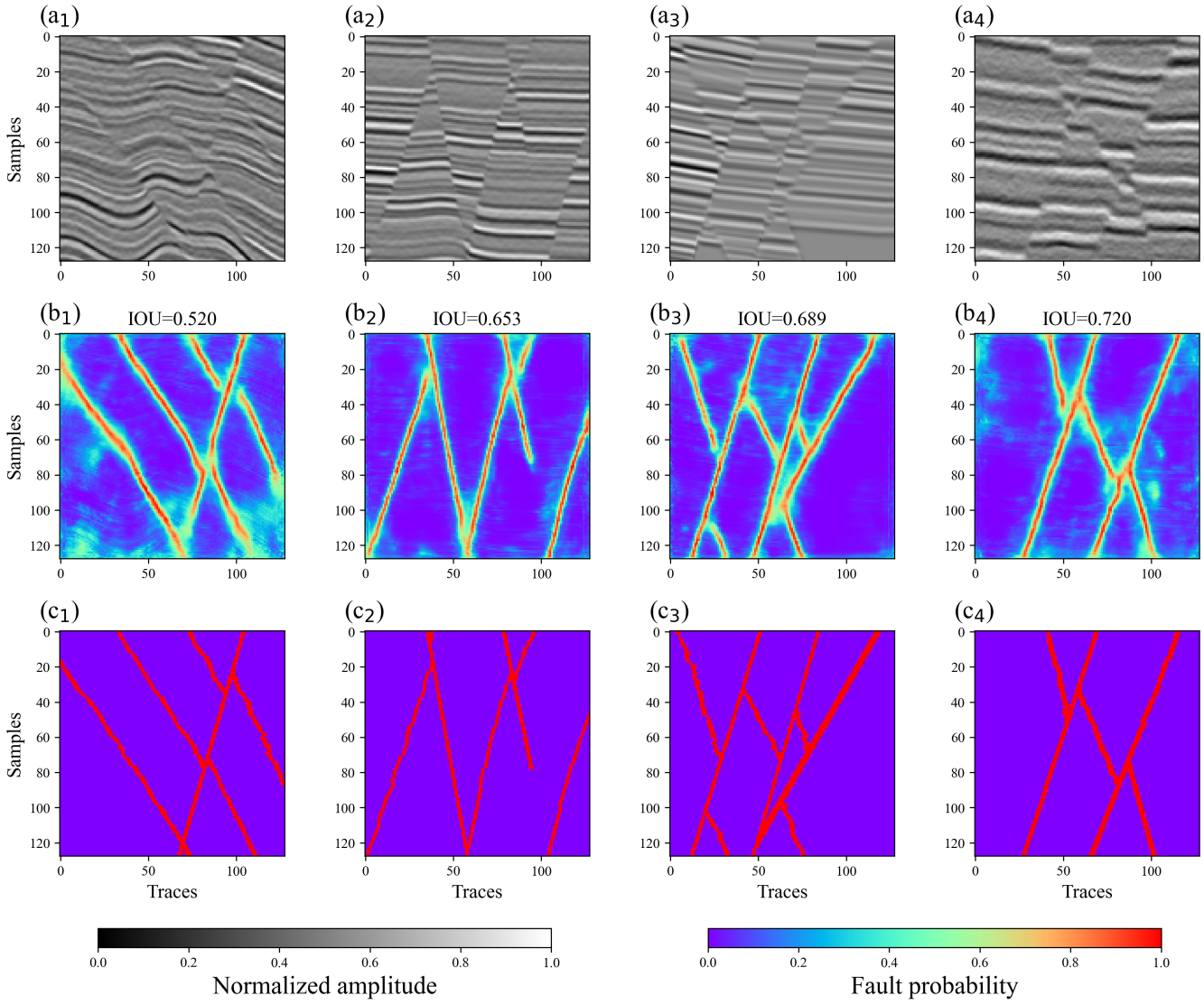

Fig. S4. (a_{1-4}) Four normalized seismic images. (b_{1-4}) Fault probability predicted by FaultNet. (c_{1-4}) Corresponding fault labels.

References

1. FJ Provost, T Fawcett, R Kohavi, , et al., The case against accuracy estimation for comparing induction algorithms. in *ICML*. Vol. 98, pp. 445–453 (1998).

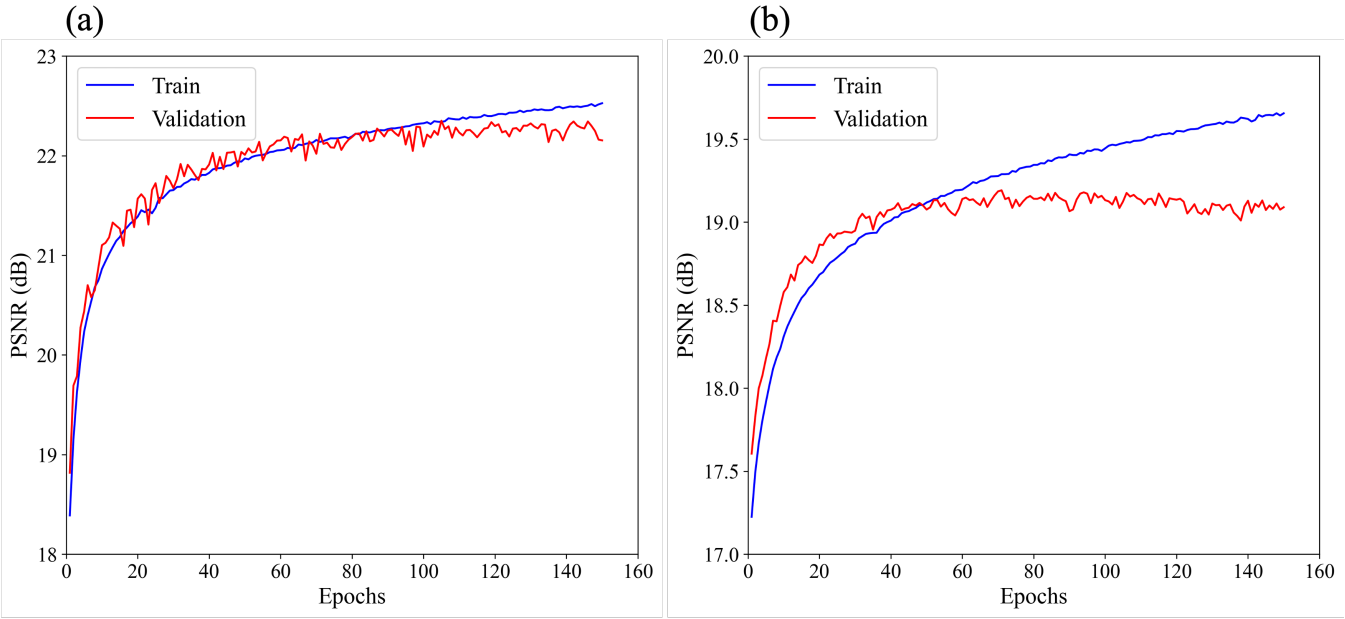

Fig. S5. The variation of PSNR during the training of $4\times$ (a) and $8\times$ (b) seismic image super-resolution.